MESO-SCALE PROCESS MODELLING STRATEGIES FOR PULTRUSION OF UNIDIRECTIONAL PROFILES

Onur Yuksel[1,2,4], Ismet Baran[1,5], Filip Salling Rasmussen[3], Jon Spangenberg[3], Nuri Ersoy[2], Jesper H. Hattel[3] and Remko Akkerman[1]

[1]Chair of Production Technology, Faculty of Engineering Technology, University of Twente, NL-7500AE, Enschede, The Netherlands
[2]Mechanical Engineering Department, Bogazici University, 34342, Istanbul, Turkey
[3]Technical University of Denmark, Mechanical Engineering Department, DK-2800 Kgs. Lyngby, Denmark
[4]Email: o.yuksel@utwente.nl
[5]Email: i.baran@utwente.nl

Keywords: Pultrusion, fiber distribution, process model, permeability, residual stress

Abstract
The resin injection pultrusion is an automated composite manufacturing method in which the resin is injected in a chamber. The flow and the thermo chemical mechanical (TCM) models have been studied for the pultrusion process to improve the reliability of the final products. Flow models are needed to understand and describe the fiber impregnation, filling time and presence of dry spots or voids. Also pressure field in the injection chamber can be estimated with flow models. TCM models are needed to predict residual stress distributions and to optimize the process conditions. A non-uniform fiber distribution strongly affects the results of both types of models. In this study, different strategies are carried out to implement non-uniform fiber distributions into the models. The cross-sectional image and fiber distribution of a 19×19 mm glass fiber reinforced polyester unidirectional pultruded composite is used. Non-uniform fiber distribution is observed and implemented into the flow model by means of permeability variations. The results of this study are compared with uniform fiber distribution results. In the TCM model, the non-uniform fiber volume content is implemented within different sized patches. The results show that the non-uniform fiber fraction should be taken into account for the process models of composites in order to capture the local process induced stresses and probability of dry spots or voids due to poor fiber impregnation.

1. Introduction

Resin injection pultrusion (RIP) is one of the most convenient composite manufacturing methods for mass production of constant cross-sectional profiles. The technique itself is very promising to manufacture a variety of products with less labor power, energy cost, and higher fiber volume fraction. There are two main sections in RIP: the first one is the resin injection chamber in which the fiber reinforcements are impregnated, and the second one is the heating section of the die in which the thermosetting resin is cured. The schematic view of a RIP is seen in Figure 1(a). To increase the overall quality of fiber reinforced polymer composites produced by the RIP process, mechanisms occurred in both of the sections should be understood. The local fiber distribution is one of the most influential parameters for a proper resin flow through the fiber reinforcements as well as for the residual stresses taking place in the pultruded part. The permeability of fibers and hence the resin flow front advancement through the fiber reinforcements are influenced by the local fiber distribution. Similarly, the effective thermomechanical properties together with the chemical shrinkage of the resin during curing are

dependent on the local fiber distribution and content which eventually affect the process induced residual stresses.

The resin flow inside the pultrusion die has been investigated for decades. Mainly the pressure field in the injection die, the backflow and the complete wet out time were investigated numerically [1-4] and validated with experimental studies in [5]. In [6], the effect of fiber volume fraction on localized fiber compaction was investigated. The fiber compaction near the resin injection ports which caused an increase in the local fiber volume fraction was included in the process models in [6]. The influence of non-uniform fiber distribution through the cross-section and the resin rich regions on the meso-scale flow have not, to the best of our knowledge, been studied for pultrusion process.

Apart from the resin flow models, the TCM models have been developed specifically for pultrusion in order to predict the temperature, cure and stress/strain developments during the process. The residual stress field should be predicted accurately for the sake of estimating the structural limits of composite parts for different loading scenarios. In [7], a novel process model was proposed to predict the stress field occurring in pultrusion and used in [8-10] to estimate the process induced residual stress level for different geometries such as rectangular shape [8], L-shaped [9] and an airfoil cross section [10]. In general, the process models include thermal, chemical and mechanical analysis with intrinsic and extrinsic interactions. Mostly uniform fiber distribution has been assumed to decrease the complexity, and macro scale analysis has been held in process models. In a recent study in [11], the local effect of non-uniform fiber distribution was investigated for the pultrusion of a glass/polyester profile and it was concluded that the proposed process modeling framework was efficient to predict the local residual stress evolution during processing. Only a local area with non-uniform fiber distribution was considered in [11] and the effect of actual fiber distribution on the residual stresses over the whole cross section was not reported. This might be useful for interpreting the measured residual strains from the hole drilling with digital image correlation experiments recently reported in [12].

The main aim of this study is to investigate the effects of the non-uniform fiber distribution on the residual stress as well as inter-tow and intra-tow resin flow. Firstly, the image process for fiber detection and the method used for resin-rich region recognition are explained and applied to the investigated profile. The effect of non-uniform fiber distribution through the whole cross section of a pultruded glass/polyester with a cross section of 19×19 mm is investigated in the TCM model as seen in Figure 1(b). The process model proposed in [7] is used for the TCM model to understand the effect of non-uniformity on residual stress arising from the process. Non-uniform fiber distribution is implemented with unit square patches for which the fiber volume fractions are analyzed independently [13]. The difference between predicted stress values for different patch sizes is presented briefly. A two dimensional (2D) Darcy model proposed in [14] is used for the resin flow through the thickness direction developed in order to capture the inter- and intra-tow resin flow. The quarter of the whole cross section which is shown in Fig. 1(b) (approximately 8×8 mm) is considered in the flow simulations for the sake of computational time. The behaviour of the resin flow for uniform, non-uniform, and non-uniform with continuous resin rich region fields are presented and discussed.

2. Image processing

Optical microscopy images of a unidirectional glass fiber reinforced polyester pultruded profile were captured with a Keyence VHX 5000 digital microscope. Nearly the whole cross section was obtained in 4 pieces with the stitching option of the microscope. After the images were taken, the individual fibers were detected in MATLAB with the built-in function '*imfindcircles*'.The detected fibers were assigned to zero and the remaining parts were assigned to one in the array of captured image. Subsequently, the fiber volume fractions for different size of patches were calculated by an area averaging for the cross-section indicated in Fig. 1(b) with red solid line. One quarter of the whole cross section can be seen in Fig. 2(a) and the fiber volume fraction distribution for the same quarter (seen in Fig. 1(b)) with different patch sizes can be seen in Fig. 2(b). Average fiber volume fraction for the flow domain and TCM domain seen in Fig. 1(b) were estimated as 0.483 and 0.487, respectively.

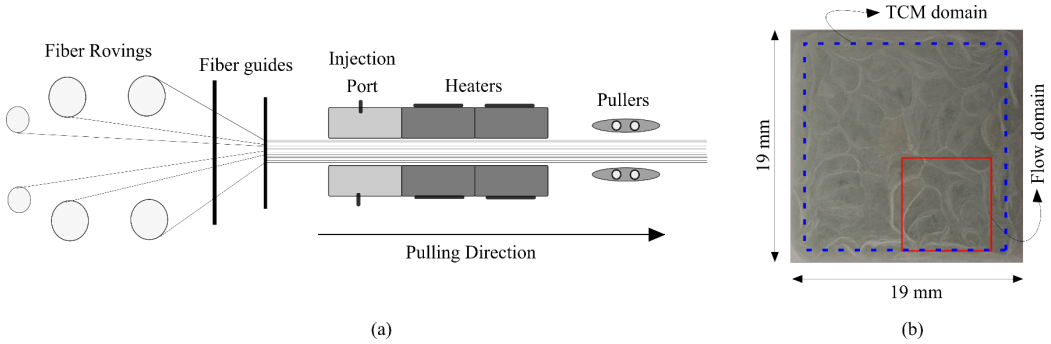

Figure 1. A schematic representation of resin injected pultrusion process (a), cross sectional view of the investigated pultruded profile with the regions investigated in the flow model (red solid) and the TCM model (blue dashed) (b)

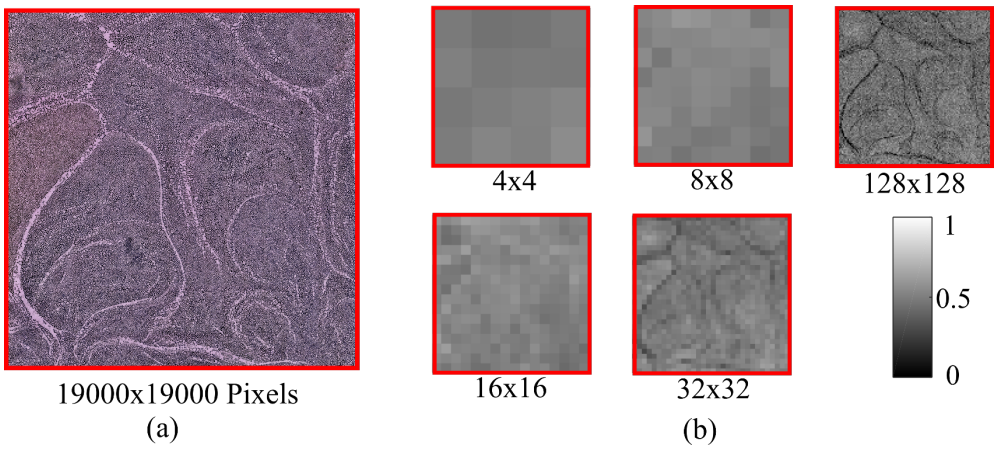

Figure 2. Fiber distribution investigation. (a) Optical microcopy image of the region investigated in the flow model. (b) Fiber volume fraction distribution with different patch sizes, i.e. pixel size, for the corresponding part of the cross section.

An efficient resin rich region characterization is specifically important for a computationally fast resin flow modeling through fibers. To automatize the resin rich region recognition from the microscopy images, all the neighboring fibers of each fiber were detected and labelled. The first six closest neighboring fibers for each fiber were listed in an array. The resin rich regions can be detected with different criterion based on the distance between neighboring fibers with the assumption of square and hexagonal periodic distribution. The flow chart of the detection procedure for the neighboring fibers is shown in Fig. 3(a). In the present study, the fibers having a distance more than 70 and 90 pixels to their fifth and sixth furthest fiber, respectively, were listed in a different array as adjacent to the resin rich areas. The fibers that were detected as “near resin rich regions” based on the proposed procedure for neighboring fiber detection can be seen in Fig. 3(b) and (c). As a last step, to implement the pure resin dominated regions with very low fiber content into the flow model, the detected fibers were connected with Delaunay triangulation and the triangles which have edge length longer than 550 pixels were discarded to capture the connection between continuous resin rich areas. The fiber volume fraction of the elements which are inside the remaining Delaunay triangles were taken as 0.05 in the flow model. The approach shown in Fig 3 yielded in representation of the realistic effect of resin rich regions using a computationally fast framework, i.e. the relatively large element size is used.

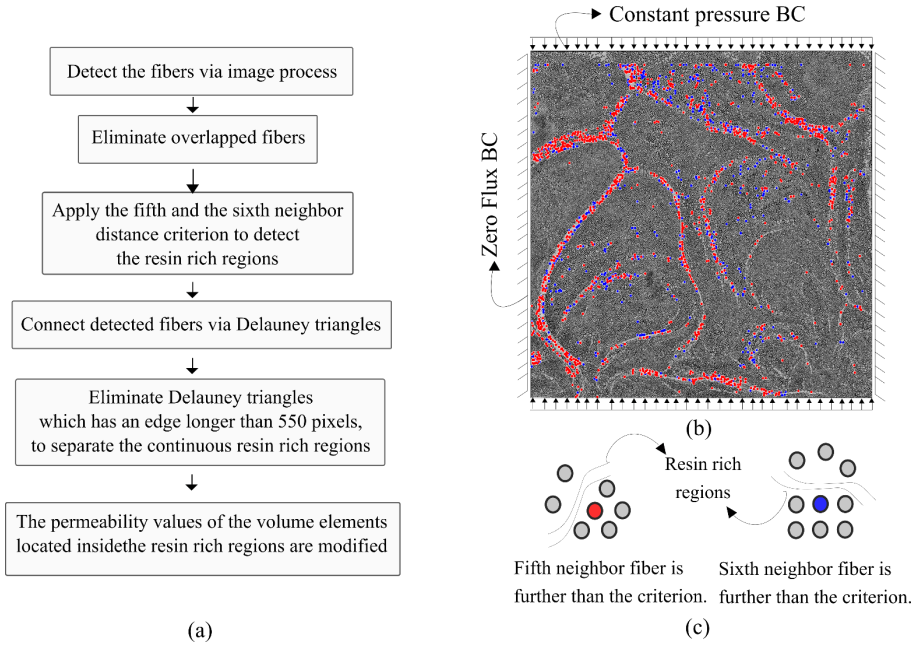

Figure 3. Flow chart of the resin rich region recognition (a), detected fibers near resin rich regions (b), the method for automatized resin rich region recognition (c)

3. Pultrusion Process Model

Non-uniform fiber distributions presented in Section 2 were implemented into the flow and TCM models with different approaches. It is noteworthy that these models are simple models and developed for quantitative estimation of the effect of non-uniform fiber distribution on the flow behavior and residual stress formation. For instance, the advection term in the flow and heat transfer model was not included because of the simplified 2D approach through the cross section. These models can be improved as independent process models for pultrusion process in the future.

3.1. Flow Model

A finite element/nodal volume technique with Darcy flow proposed in [14] was implemented in the present study in order to investigate the 2D resin flow front advancement through the cross section of the pultruded profile. An in-house flow solver was developed in MATLAB for this purpose. To isolate the effect of resin rich regions on the flow advancement, the flow through the axial direction was neglected and the resin was assumed to be incompressible. Hence, the governing equation for the 2D Darcy flow can be written as [14]:

$$\frac{\partial}{\partial x}\left(\frac{K_x}{\mu}\frac{\partial P}{\partial x}\right)+\frac{\partial}{\partial y}\left(\frac{K_y}{\mu}\frac{\partial P}{\partial y}\right)=0 \quad (1)$$

Where K_x and K_y are the components of the permeability tensor, P is the resin pressure and μ is the resin viscosity. As the simplified version of the real case, constant pressure was defined as the boundary condition for the top and the bottom surfaces and zero-flux wall for the side surfaces as seen in Fig. 3(b). Note that the fiber volume fraction dependent permeability was defined with the modified Kozeny-Carman equation as a heuristic model which is given in Eq. 2 [15]:

$$K_x = K_y = \frac{{R_f}^2}{4k'} * \frac{(\sqrt{{V'}_a/V_f} - 1)^3}{({V'}_a/V_f + 1)} \quad (2)$$

where the transverse permeability values K_x and K_y are dependent on empirical parameters ${V'}_a$ and k', R_f is the average fiber radius and V_f is the fiber volume fraction. Continuity is obtained by the following equation:

$$\frac{\partial}{\partial t}\int_{\Omega} f\ \phi \cdot d\Omega - q = 0 \quad (3)$$

where f is the resin concentration for a small volume Ω which can also be mentioned as fill factor. Φ is the porosity value and q is the resin flow rate. The details of the free surface algorithm and associated boundary conditions can be found in [14]. After the continuous resin rich regions were implemented into flow model, average fiber volume fraction through the modelled domain was reduced from 0.487 to 0.382. To have a reasonable comparison, average fiber volume fractions of the other cases were equalized.

3.2. Thermo Chemical Mechanical Model

As the simplified version of the pultrusion process model, a coupled temperature displacement analysis was carried out using the commercial finite element software package ABAQUS for the region shown in Fig. 1(b) with blue dashed lines. A 2D TCM model was developed and an 8-node plane strain thermally coupled quadrilateral element was used (biquadratic displacement, bilinear temperature, reduced integration - CPE8RT). Element sizes were same for each model. The temperature of the pultrusion die was taken from [9], i.e. two heaters at 110˚C and 140˚C, and implemented with prescribed temperature profile at the boundaries. The temperature at the outer boundaries was defined with respect to the pulling rate equal to 150 mm/min, i.e. it takes 400 s for the cross section to pass the pultrusion die of 1 m. The heat generation term was calculated with respect to the curing and fiber volume fraction in HETVAL subroutine in ABAQUS with the curing kinetics parameters given in [16]. The fiber volume fraction dependent thermal expansion coefficient and cure shrinkage were determined in UEXPAN subroutine. The mechanical properties, which are also cure and temperature dependent, was defined in UMAT subroutine. The further details of the implementation of TCM model can be found in [7]. The Self-Consistent Field Micromechanics is used to handle corresponding material properties. The convective cooling to the ambient temperature was applied to the outer boundaries of the model geometry.

4. Results

The flow model was carried out for the one quarter of the cross section that can be seen in Fig. 3(b) as aforementioned. The results for the uniform fiber volume fraction, non-uniform fiber volume fraction through the cross section and non-uniform field with specific resin rich regions defined as high permeable continuous regions were compared with respect to filling time and resin flow front advancement through the process. The TCM model was carried out for the non-uniform fiber volume fraction through the whole cross section with changing patch sizes. One quarter of the field with changing patch size can be seen in Fig. 2(b)

4.1. Flow Model Results

The implemented fiber volume fraction fields and flow front for different time steps can be seen in Fig. 4 with the overall V_f per case. The complete filling times were calculated as 1.65, 1.86 and 1.64 s for uniform, non-uniform and continuous permeable resin rich region cases, respectively. It is shown that the filling time is longer for the non-uniform fiber volume fraction distribution. On the other hand, when the nodes for resin rich regions are modified with high permeability, those areas behave as a resin distribution layer around the tows. Resin rich region modification is decreasing the estimated filling time with respect to the non-uniform distribution approach. In addition, the closed dry regions were found to formed during the flow front progress. However, this might not be the case in 3D because the entrapped air can escape from the back side of the injection chamber. It should be noted that the fibers can also be misaligned in the structure which prevents air escape. causing fluctuation through the axial direction and might lead air entrapment. For a detailed investigation of the misalignment and porosity in a pultruded part [17] can be referred.

4.2. Thermo Chemical Mechanical Model Results

The predicted residual stress field for different patch sizes can be seen in Fig. 5 with the corresponding fiber volume fraction distributions. The maximum predicted stress values were found to increase with a decrease in the patch size. This phenomenon can be explained by the increase in mismatch in mechanical properties as well as chemical shrinkage during curing with higher resolution of the patch. The maximum transverse normal stress computed for the smallest patch size was found to be approximately 8.7 MPa and 7.4 MPa in the X- and Y-axis, respectively. It is noteworthy that the minimum V_f for the smallest patch size case was 0.338.

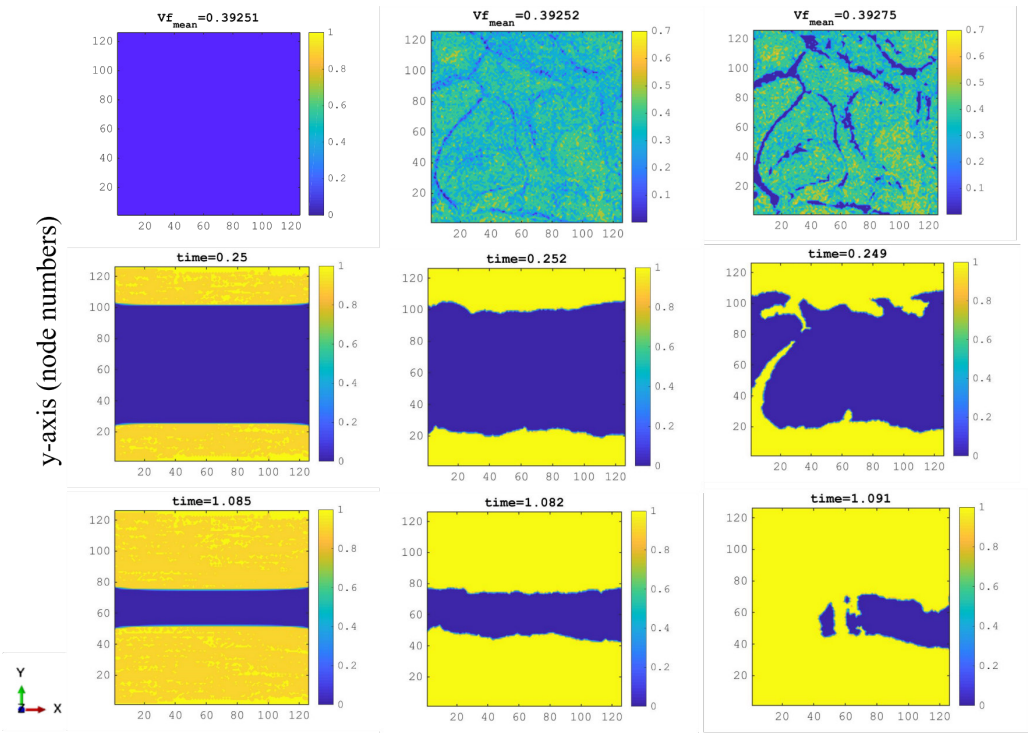

Figure 4. Flow front positions for the corresponding fiber distributions and time. (Uniform V_f (left column), Non-uniform V_f (middle column), Low V_f for resin rich regions (right column)). Investigated domain is shown in Fig. 1(b)

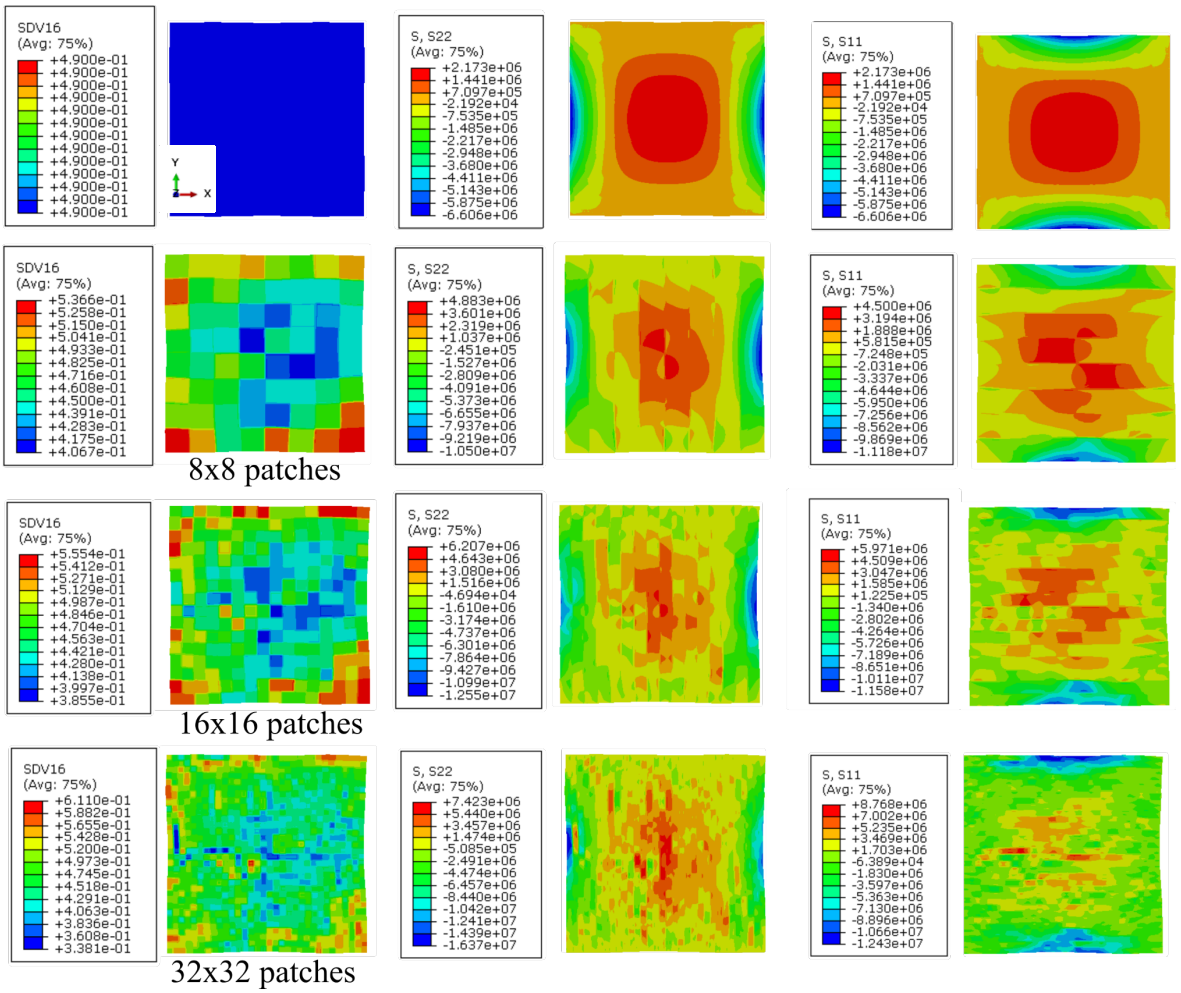

Figure 5. Predicted residual stress field for uniform and non-uniform V_f with different patch sizes. (Corresponding fiber volume fraction distributions (left column), stress in Y direction (middle column), stress in X direction (right column)). The corresponding domain for the TCM model can be seen in Fig. 1(b).

5. Conclusions

Different strategies for the implementation of non-uniform fiber distribution through the cross section were carried out for both the flow and the TCM models developed for pultrusion process of the unidirectional composite. It was shown that non-uniform fiber distribution through the cross section can result in higher filling time which should be taken into consideration for the flow process models of pultrusion. High permeability implementation for the resin rich regions showed that inter-tow gaps were filled with resin at first. Pressurized resin around the tow can push fibers to the center of tows which can lead to lower localized permeability and insufficient impregnation of the core of the tows. The TCM models with non-uniform fiber distribution in different size of patches showed that the resultant stress values can be higher than the estimated values with uniform fiber volume fraction through the cross section due to an increase in the mismatch in mechanical properties and cure shrinkage. This information is valuable to use in structural applications of the composites.

The TCM model with non-uniform V_f for the whole domain predict the local residual stress distributions. This might be useful for validation of the model through hole drilling with DIC where a scatter was

obtained in [12]. The 2D Darcy flow model with non-uniform V_f distribution is shown to have the potential for capturing the possible air entrapment in the roving layer as shown in Fig. 4. In the future, it is planned to compare numerical results for different patch sizes with experimental observations.

Acknowledgment

This work is part of the project named 'Modelling the multi-physics in resin injection pultrusion (RIP) of complex industrial profiles' which has been granted by the Danish Council for Independent Research | Technology and Production Sciences (DFF/FTP), Grant no. DFF- 6111-00112.

References

[1] J. Spangenberg, M. Larsen, R.R. Rodríguez, P.M.M. Sánchez, F.S. Rasmussen, M.R. Sonne, and J.H. Hattel. The effect of saturation on resin flow in injection pultrusion: a preliminary numerical study. *Proceedings of the* 21st *International Conference on Composite Materials ICCM-21, Xi'an, China,* 2017.
[2] J.G. Vaughan, B.K. Ranga, J.A. Roux and A.L. Jeswani. Effect of injection chamber length and pull speed of tapered resin injection pultrusion. *Journal of Reinforced Plastics and Composites*, 30(16):1373-1387, 2011.
[3] S. S. Rahatekar and J. A. Roux. Numerical simulation of pressure variation and resin flow in injection pultrusion. *Journal of Composite Materials*, 37(12):1067-1082, 2003.
[4] P. Simacek and S.G. Advani. Simulating tape resin infiltration during thermoset pultrusion process. *Composites Part A: Applied Science and Manufacturing*, 72:115-126, 2015.
[5] Z. Ding, S. Li, H. Yang, L.J. Lee, H. Engelen, and P.M.(Mac) Puckett. Numerical and experimental analysis of resin flow and cure in resin injection pultrusion (RIP). *Polymer Composites*, 21(5):762-778.
[6] N.B. Masuram, J.A. Roux, and A.L. Jeswani. Resin viscosity influence on fiber compaction in tapered resin injection pultrusion manufacturing. *Applied Composite Materials*, 25(3):485-506, 2018.
[7] I. Baran, C.C. Tutum, M.W. Nielsen, and J.H. Hattel. Process induced residual stresses and distortions in pultrusion. *Composites Part B: Engineering*, 51:148-161, 2013.
[8] I. Baran, J.H. Hattel, and R. Akkerman. Investigation of process induced warpage for pultrusion of a rectangular hollow profile. *Composites Part B: Engineering*, 68:365-374, 2015.
[9] I. Baran, R. Akkerman, and J.H. Hattel. Modelling the pultrusion process of an industrial l-shaped composite profile. *Composite Structures*, 118:37-48, 2014.
[10] I. Baran, C.C. Tutum, and J.H. Hattel. The internal stress evaluation of pultruded blades for a darrieus wind turbine. In The Current State-of-the-Art on Material Forming, volume 554 of Key Engineering Materials, pages 2127-2137. Trans Tech Publications, 7 2013.
[11] I. Baran. Analysis of the local fiber volume fraction variation in pultrusion process. *AIP Conference Proceedings*, 1896, 030029, 2017.
[12] O. Yuksel, I. Baran, N. Ersoy, and R. Akkerman. Analysis of residual transverse stresses in a thick ud glass/polyester pultruded profile using hole drilling with strain gage and digital image correlation. *AIP Conference Proceedings*, 1960, 020040, 2018.
[13] S.H.R. Sanei and R.S. Fertig. Uncorrelated volume element for stochastic modeling of microstructures based on local fiber volume fraction variation. *Composites Science and Technology*, 117:191-198, 2015.
[14] X.L. Liu. A finite element/nodal volume technique for flow simulation of injection pultrusion. *Composites Part A: Applied Science and Manufacturing*, 34(7):649-661, 2003.
[15] T.G. Gutowski, Z. Cai, S. Bauer, D. Boucher, J. Kingery, and S. Wineman. Consolidation experiments for laminate composites. *Journal of Composite Materials*, 21(7):650-669, 1987.
[16] I. Baran, R. Akkerman, and J.H. Hattel. Material characterization of a polyester resin system for the pultrusion process. *Composites Part B: Engineering*, 64:194-201, 2014.
[17] I. Baran, I.Straumit, O. Shishkina, and S.V. Lomov. X-ray computed tomography characterization of manufacturing induced defects in a glass/polyester pultruded profile. *Composite Structures*, 195:74-82, 2018.